

TECHNICAL REPORT

SUPPLEMENTAL ELECTRICAL RESISTIVITY SURVEYS
ASCENSION ISLAND
SOUTH ATLANTIC OCEAN

Prepared For

UNITED STATES AIR FORCE
EASTERN SPACE AND MISSILE CENTER
PATRICK AIR FORCE BASE,
FLORIDA

And

UNITED STATES DEPARTMENT OF ENERGY
IDAHO FALLS OPERATIONS OFFICE
IDAHO FALLS, IDAHO

OCTOBER 26, 1984

SUPPLEMENTAL
ELECTRICAL RESISTIVITY SURVEYS

ASCENSION ISLAND
SOUTH ATLANTIC OCEAN

Prepared for

United States Air Force
Eastern Space and Missile Center
Patrick Air Force Base, Florida 32925

and

United States Department of Energy
Idaho Falls Operations Office
Idaho Falls, Idaho

by

Earth Science Laboratory
University of Utah Research Institute

Howard P. Ross
Claron E. Mackelprang
Sharrif F. Dajany

October 26, 1984

NOTICE

This report was prepared to document work sponsored by the United States Government. Neither the United States nor its agent, the United States Department of Energy, nor any Federal employees, nor any of their contractors, subcontractors or their employees, makes any warranty, express or implied, or assumes any legal liability or responsibility for the accuracy, completeness, or usefulness of any information, apparatus, product or process disclosed, or represents that its use would not infringe privately owned rights.

NOTICE

Reference to a company or product name does not imply approval or recommendation of the product by the University of Utah Research Institute or the U.S. Department of Energy to the exclusion of others that may be suitable.

CONTENTS

	<u>Page</u>
1.0 EXECUTIVE SUMMARY.....	1
2.0 INTRODUCTION.....	2
3.0 GEOLOGY.....	2
4.0 GEOPHYSICS.....	4
4.1 Geophysical Data Base.....	4
4.2 Electrical Resistivity Survey Method.....	5
4.3 1983 Resistivity Survey.....	6
4.4 Supplemental Resistivity Surveys.....	14
Line 4.....	14
Line 5.....	16
Bipole-dipole Transmitter 6.....	16
4.5 Numerical Model Interpretation.....	16
Line 4.....	16
Line 5.....	20
Line 2.....	20
5.0 SUMMARY AND RECOMMENDATIONS.....	24
6.0 ACKNOWLEDGEMENTS.....	25
7.0 REFERENCES.....	25
APPENDIX - NUMERICAL MODEL RESULTS.....	27

ILLUSTRATIONS

Figure 1. Location of Ascension Island, the Mid-Atlantic Ridge, and ocean-fracture zones.

Figure 2(a). Bipole-dipole array geometry as used in the reconnaissance resistivity survey.

2(b). Dipole-dipole array geometry used for detailed surveys.

Figure 3. Dipole-dipole resistivity data, Line 2.

Figure 4. Dipole-dipole resistivity data, Line 3.

Figure 5. Location Map, Line 4 and 5 and Tx6 receiver sites.

Figure 6. Dipole-dipole resistivity data, Line 4.

Figure 7. Dipole-dipole resistivity data, Line 5.

Figure 8. Interpretation map, low resistivity zone.

Figure 9. Best fit numerical model solution, Line 4.

Figure 10. Best fit numerical model solution, Line 5.

PLATE I. Electrical Resistivity Survey, Ascension Island, South Atlantic Ocean

PLATE II. Electrical Resistivity Sections, Ascension Island, South Atlantic Ocean

1.0 EXECUTIVE SUMMARY

This report describes an electrical resistivity survey completed in September of 1984 as an extension of the Phase II evaluation of the geothermal potential of Ascension Island. This electrical resistivity work had been recommended to assist in siting a deep temperature-gradient hole after Phase II thermal gradient results were found to be permissive and favorable for the occurrence of a high-temperature geothermal resource.

Reconnaissance electrical resistivity measurements had been completed earlier which covered the central 35 sq km of the island. A broad zone of low apparent resistivity was mapped which trends north-northeast from Devil's Riding School through Thistle Hill. Areas west of Spoon Crater and northeast of Thistle Hill showed the lowest apparent resistivities within this broad (2 km by 5 km) zone.

Two dipole-dipole profiles which were completed in June 1983 have refined the location, depth and intrinsic resistivity of the low resistivity zones. The profiles showed high resistivities above sea level, with some resistive masses extending to considerable depth. Low-resistivity zones at depth are thought to result from sea water incursion within a few kilometers of the coast. Geothermal brines probably contribute to low-resistivity zones further inland, i.e. from Devil's Riding School to McTurk's Culvert, and south of Thistle Hill. The low-resistivity zones were incompletely defined due to rough topography, limited access and surface rocks of high electrical impedance. The low-resistivity areas as defined by the survey work were recommended for thermal gradient test drilling in a subsequent exploration effort.

Dipole-dipole lines 4 and 5 have further delineated the low-resistivity zone and will contribute to the optimum siting of deep thermal gradient tests

and a production well. Numerical modeling of lines 2, 4, and 5 and an integration of pre-existing data, suggest a zone of 5-10 ohm-m resistivities which may be associated with thermal fluids at approximately sea level depths.

2.0 INTRODUCTION

The geothermal energy potential of Ascension Island is being evaluated to determine the feasibility of a low-cost, renewable energy alternative for United States facilities at Ascension Auxiliary Airfield (Ascension AAF).

The program to this point in time has been summarized in Nielson et al. (1984). Previous geothermal exploration activities have resulted in the discovery of a geothermal system in the Middleton Ridge area. The purpose of this study is to define the lateral and vertical extent of the system so that a drill hole can be sited to collect data on temperature, rock permeability, and fluid chemistry of the geothermal system.

3.0 GEOLOGY

Ascension Island is located about 100 km west of the Mid-Atlantic Ridge median valley and 50 km south of the Ascension fracture zone (van Andel et al., 1973), as shown in Figure 1. As described by Nielson and Sibbett (1982), the island is composed almost entirely of volcanic rocks, and is the top of a volcanic mountain which rises 4 km above the sea floor and is perhaps 50 km in diameter at its base.

Nielson and Sibbett (1982) present a detailed geologic map of Ascension Island, describe the units and structures in detail, and discuss the geologic history of the island. The geophysical surveys were conducted to extend the geologic data to depth and to search for physical properties indicating a geothermal system at depth. A brief review of the geology is useful as a

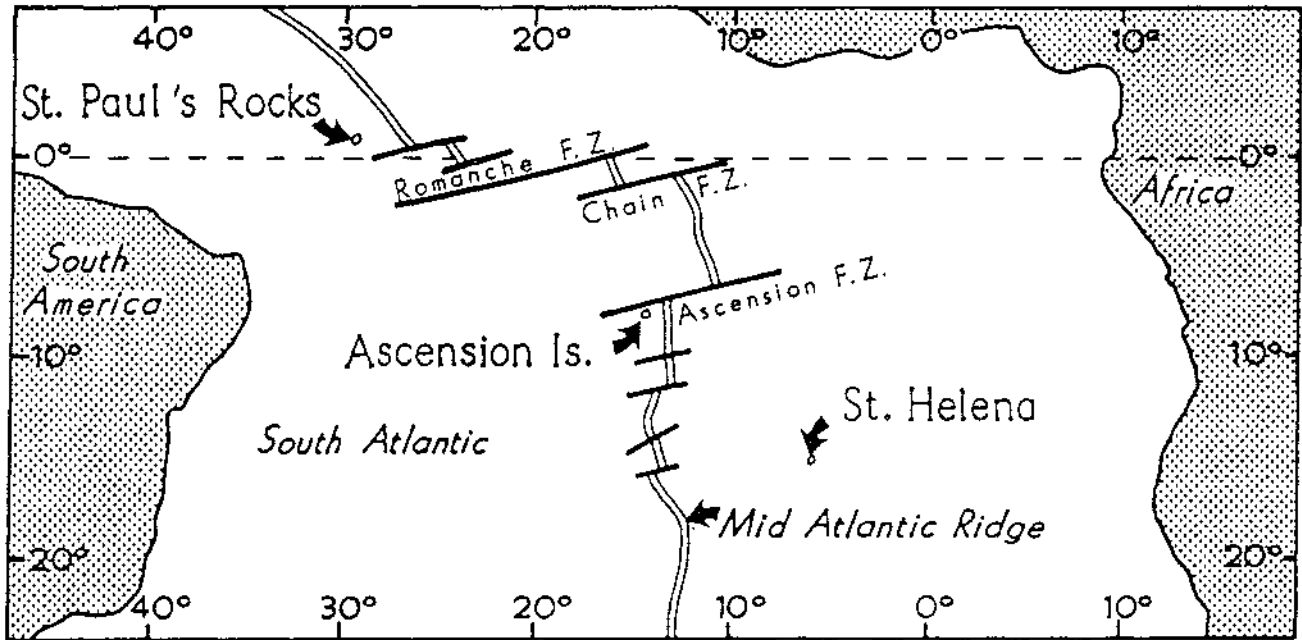


Fig. 1. Location of Ascension Island, the Mid-Atlantic Ridge and ocean fracture zones.

prelude to discussing the electrical resistivity survey.

Basalt flows dominate the surface of Ascension Island, with the youngest flows emanating from the Sisters Peak and South Gannett Hill areas. Nielson and Sibbett (1982) suggest that these flows are probably several hundred years old based on the lack of weathering and erosion. These flows cap older flows which occur throughout the island. Trachyte lava flows, pyroclastic deposits, domes and intrusions dominate the central and eastern portions of the island. Age dating suggests that the Bears Back dome was emplaced approximately 610,000 years ago. The Middleton Ridge rhyolite flow, exposed at the base of the Green Mountain stratigraphic sequence, was dated at approximately 0.94 m.y. Prominent cinder cones and cinder aprons occur throughout the island.

The young age of the basalt flows precludes the development of a significant soil profile for most of the island. Without soils and fine-grained erosional deposits to retain moisture, the basalt flows and trachytes present a very high electrical impedance near-surface environment in which injection of current into the ground for electrical geophysical surveys was found to be difficult. Nielson and Sibbett (1982) also mapped several areas of alluvial deposits, which, although generally of limited extent, were very important to the completion of the electrical resistivity surveys because current could be easily injected in these areas.

4.0 GEOPHYSICS

4.1 Geophysical Data Base

Nielson and Sibbett (1982) completed geologic mapping of Ascension Island and recommended aeromagnetic and resistivity surveys and thermal gradient drilling as a Phase II geothermal exploration program. The aeromagnetic survey was completed in March 1983 and is reported by Ross et al. (1984a). The

initial electrical resistivity survey was completed in 1983 and is reported by Ross et al. (1984b).

4.2 Electrical Resistivity Survey Method

The electrical resistivity geophysical method is used to measure the earth's resistivity, i.e. the ease with which the ground conducts electricity. High resistivity values indicate poor conductivity whereas low resistivity values indicate good conductivity. In the earth, electricity flows in the ground water because of the movement of dissolved chemical ions (salts). Most rock-forming minerals themselves do not conduct electricity. Soil moisture is held both in pore spaces between mineral grains and within and adjacent to clay minerals; thus parameters that can cause changes in measured resistivity include:

1. Porosity and permeability of the ground
2. Amount of water in the ground (percentage of saturation)
3. Amount and type of dissolved salts
4. Amount and nature of other fluids in the ground
5. Amount and nature of clay minerals present.

Geothermal waters usually have a higher concentration of dissolved chemical constituents than normal ground water as well as high temperatures and thus cause a lower earth resistivity. Zones of clay alteration in the earth can often be detected and mapped by the low resistivity values associated with them.

Earth resistivity changes caused by thermal fluids and clays are mapped at the surface by deploying a system of four electrodes. A precisely controlled current is injected into the ground between two current electrodes, and a resulting voltage is measured between two potential electrodes. The measured voltage is a function of the geometrical parameters of the electrode

array, the magnitude of the injected current and the resistivity structure of the surrounding earth. An apparent electrical resistivity can be calculated from the formula,

$$\rho_a = \frac{\Delta V}{I} \times Q,$$

where I = current introduced, ΔV = measured voltage, and Q is the geometric array factor. This apparent resistivity would be the true value of resistivity if there were no lateral or vertical variations in actual earth resistivity. But since the actual resistivity does vary, the apparent resistivity is a kind of average of all the variations. To perform a survey, values of apparent resistivity are measured at a number of points at the surface of the earth. Computer-assisted interpretation of the set of resistivity data is then undertaken to construct a picture of true resistivity variations in the subsurface. This picture of subsurface resistivity variation is then interpreted in terms of variations in rock type, alteration, and fluid salinity.

4.3 1983 Resistivity Survey

Electrical resistivity surveys completed in June 1983 included a reconnaissance resistivity survey and three dipole-dipole profiles. The reconnaissance resistivity survey was conducted using the bipole-dipole array, which permits the most flexibility in deployment of the transmitter dipole (and hence electrodes) and the selection of receiver sites. The bipole-dipole method permits a rapid mapping of the areal distribution at the expense of resolution. It has been widely used in geothermal exploration (i.e. Keller et al., 1975; Stanley et al., 1976) even though the contoured apparent resistivity patterns are complex and difficult to interpret. Keller et al. (1977) used this method very effectively in the reconnaissance exploration for geo-

thermal resources on the East Rift Zone of Kilauea Volcano, Hawaii Island. The young basalt flows on Hawaii give rise to high electrode impedances, restricted surface access, and sea water intrusion, all problems which were expected and encountered on Ascension Island.

Figure 2a illustrates the bipole-dipole array geometry and parameters as used in this survey. A transmitter dipole length of 610 meters was chosen to provide adequate current penetration to depths of 600 to 1200 meters for receiver sites located from 600 to 3000 meters from this dipole. The resultant voltages were measured with orthogonal 152 m dipoles. An Elliot Model P-15B engine generator and Elliot Model 15 transmitter produced 3 to 5 amp of current at voltages of 200 to 300 volts, which was transmitted as a time-domain pulse of 4 seconds on followed by 0.5 seconds of current off. Voltages across the potential electrodes were measured with a Fluke Model 8050A digital multimeter. The total-field apparent resistivity was computed from the expression

$$\rho_a = [(V_1^2 + V_2^2)]^{1/2} \frac{Q}{I}$$

where V_1 and V_2 are the observed (orthogonal) voltages, I is the transmitted current, and Q is the geometric factor for the standardized dipole lengths and variable transmitter-receiver positions (Hohmann and Jiracek, 1979; Frangos and Ward, 1980). In practice, Q was interpolated from a contoured overlay chart at the scale of the topographic map (1:25,000) on which the transmitter and receiver sites had been plotted.

Transmitter sites were chosen such that electrodes could be emplaced in alluvium or weathering debris among the flows, and still result in an efficient and fairly detailed resistivity map of the island. A substantial effort was expended in electrode preparation for each transmitter dipole. The

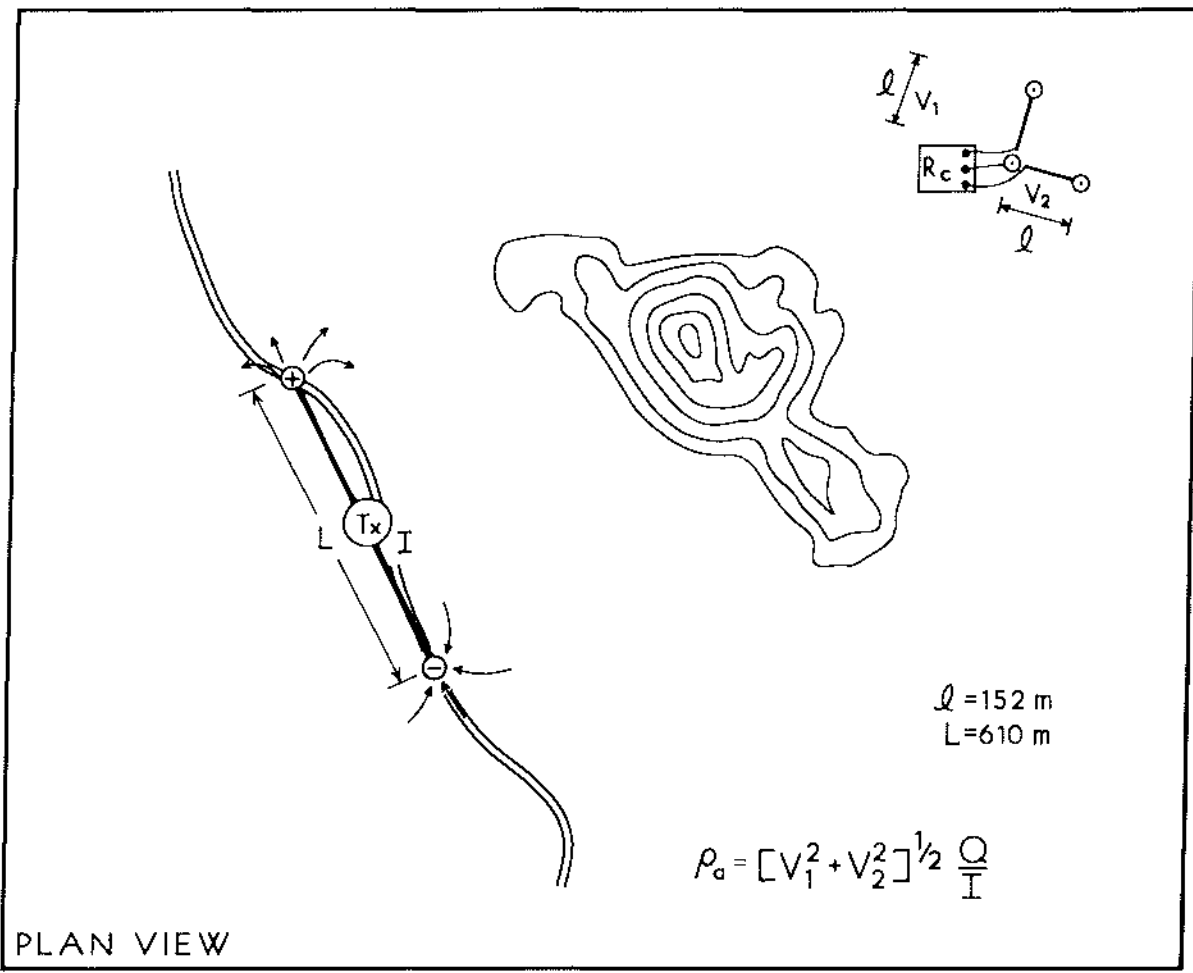


Figure 2a. Bipole-dipole array geometry as used in the reconnaissance resistivity survey.

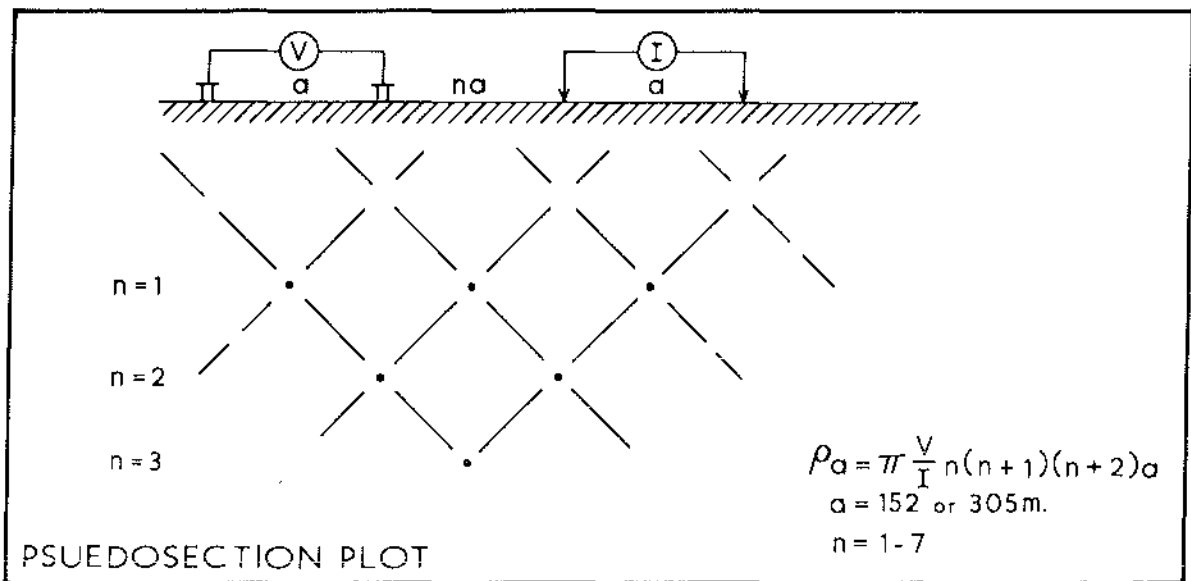


Figure 2b. Dipole-dipole array geometry used for detailed surveys.

reconnaissance resistivity survey covered an area of approximately 35 sq km in the central portion of the island. Transmitter sites within a kilometer of the coast would certainly be dominated by the 0.2-2 ohm-m current path afforded by sea water at depth and offshore, as noted by Keller et al. (1977) in their studies of the Kilauea east rift zone. Accordingly the survey was limited to the central portion of the island considered most favorable for the development of a geothermal resource. The Sisters Peak - Bears Back area was only partially covered by the survey because of poor access and high surface impedance. Transmitter-receiver separation, reduced apparent resistivity and other parameters for all stations are listed in Table 1, which has been updated to include Transmitter 6 of the September 1984 survey.

Although the interpretation of reconnaissance scale bipole-dipole data is rather qualitative and complex (Hohmann and Jiracek, 1979), low resistivity regions were identified in a cost-effective manner. The survey identified four low resistivity zones: 1) the Lady Hill-Travelers Hill-Sisters Peak area; 2) south of Devil's Riding School; 3) Grazing Valley-Hospital Hill, and 4) Cricket Valley.

Three dipole-dipole profiles were completed to obtain more detailed electrical resistivity data. The geometry and plotting scheme for this array are shown in Figure 2b. All electrodes are placed in a line, a uniform distance (separation) apart. The dipole-dipole array is widely used in geothermal, mineral and petroleum exploration because it is an efficient means of collecting a large number of data points which are influenced by both the lateral position and depth characteristics of the resistivity distribution. Numerical modeling programs can be used in a forward modeling or iterative manner to determine the resistivity distribution and the intrinsic resistivity values. The locations of the three profiles are shown on Plate I.

TABLE I
RECONNAISSANCE RESISTIVITY
DATA SUMMARY

Transmitter	Receiver	Distance (m)	I (amp)	Q	ρ_a (ohm-m)	Transmitter	Receiver	Distance (m)	I (amp)	Q	ρ_a (ohm-m)	
Tx-1 (Old Well)	1-ENE	2800	5.00	900	8.8?*	Tx-3 (Grazing Valley)	3-SE	1560	4.60	160	78.9	
	1-NNE	2060	5.00	425	9.0		3-E	1780	4.61	390	57.3	
	1-N	2030	4.90	530	18.6		3-NW	1620	4.60	260	175.8?	
	1-NW	1740	4.90	235	19.3		3-W	2120	4.65	620	< 12.3*	
	1-WNW	2440	4.90	525	15.2		3-N	1750	4.57	180	12.0	
	1-W	1820	5.00	200	11.8		2-SE	2390	4.73	600	12.0	
	1-SW-1	1820	4.90	225	15.2		3-NE	2280	4.65	400	< 34.0#	
	1-SW-2	1810	4.90	305	12.2		Tx-4 (One Boat Dump)	4-N	2420	3.85	575	19.7
	1-S	1590	4.80	275	12.6			4-NW	1220	4.20	125	7.2
	1-SE	2520	4.80	750	39.1			4-W	1340	4.13	90	82.4
	1-E	2630	4.72	600	31.9			4-SW	2360	4.06	465	12.8?*
Tx-2 (Dark Slope Crater)	2-SE	900	4.63	40	95.7	4-SE-1		1320	3.98	165	13.1	
	2-S	810	4.58	20	562	4-NE-2		3200	4.01	1300	< 9.2*	
	2-NW	1510	4.53	250	76.1	4-NE-1		2940	3.95	900	< 5.1*	
	2-NE-1	1460	4.55	95	19.4	4-NE-3	1220	3.90	60	152.0		
	2-E-1	1680	4.52	180	14.8	Tx-5 (Devil's Ashpit)	5-ENE	880	3.20	20	142	
	2-N-1	1030	4.54	50	367		5-NE	1220	3.13	85	87.7	
	2-ESE	2240	4.50	575	< 13.3*		5-N-1	960	3.10	55	66.3	
	2-NE-2	1860	4.51	210	28.7		5-N-2	1440	3.12	185	2,435	
	2-N-2	2030	4.92	350	115.2		5-NW	1480	3.10	180	379	
	2-SW	1740	4.80	175	23.1		5-W	1420	3.08	90	58.3	
					5-SW		2240	3.08	385	130		
Tx-6 (LDTGH area)	6-N	1500	3.30	240	5.5	6-NE	1240	3.31	60	4.5		
	6-NE	1240	3.31	60	4.5	6-SE	1660	3.47	195	20.0		
	6-SE	1660	3.47	195	20.0	6-S	1060	3.36	90	20.9		
	6-S	1060	3.36	90	20.9	6-W	1700	3.35	160	27.7		
	6-W	1700	3.35	160	27.7	6-NW	1800	3.29	330	19.5		
	6-NW	1800	3.29	330	19.5	6-SSE	1400	3.40	195	8.7		
	6-SSE	1400	3.40	195	8.7							

* very low signal - ρ upper bound
high noise level - ρ upper bound

Line 1 was completed to determine the suitability of an area near Command Hill for a proposed fresh water well, and to determine the resistivity layering of the first 300 m of depth.

Line 2 trends roughly north and is centered just north of the NASA road east of Devil's Riding School (Plate I). This is a line of six current electrodes spaced 305 m apart (a six-spread of 305 m dipoles). This line was sited to provide additional lateral and vertical detail on the low-resistivity zone indicated by reconnaissance resistivity measurements.

The observed data for line 2 are shown as Figure 3. Observed resistivities decrease from 100-200 ohm-m at the first separation to 10-30 ohm-m for separations 5, 6, and 7. Thus, a rough resistivity layering with depth is indicated. The lower resistivity values observed for larger separations are in excellent agreement with the reconnaissance resistivity data. The numerical model solution for these data, Plate II, shows 200 to 500 ohm-m bodies above sea level, a mix of 200 to 30 ohm-m bodies from 70-150 m below sea level and an extensive zone of 15 ohm-m below this. The 30 to 200 ohm-m bodies may represent a very thin fresh water zone and its mixing zone with sea water, and possibly geothermal waters. A 10 ohm-m zone may exist between station 1 to 4 north, as inferred by a slightly better fit to the observed data. The most prospective geothermal area, inferred from these resistivity data, would extend between stations 0 and 4 north.

Dipole-dipole line 3 (Figure 4) is centered north of an antenna array along the North East Bay road and trends approximately N15°E. Line 3 is a five-spread with 305 m dipoles. The observed data of Figure 4 indicate high (200-450 ohm-m) near surface resistivities corresponding to the alluvium and young basalt flows. These units are either very dry or the contained waters have few dissolved ions. Resistivity decreases with increased separation

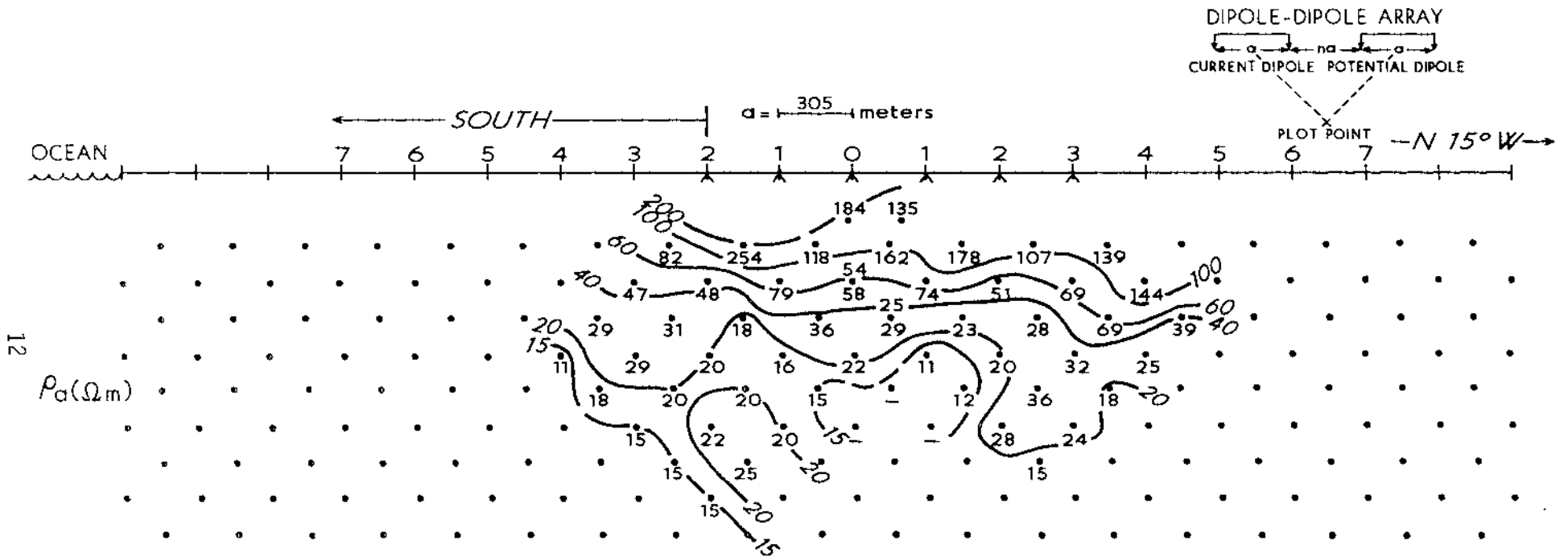


FIGURE 3
LINE 2
DIPOLE-DIPOLE ARRAY—APPARENT RESISTIVITY
TRANSMITTER: ELLIOT M15 RECEIVER: FLUKE
ASCENSION ISLAND, SOUTH ATLANTIC



DATA BY
H. P. ROSS and D. J. GREEN
JUNE 17, 18, 1983

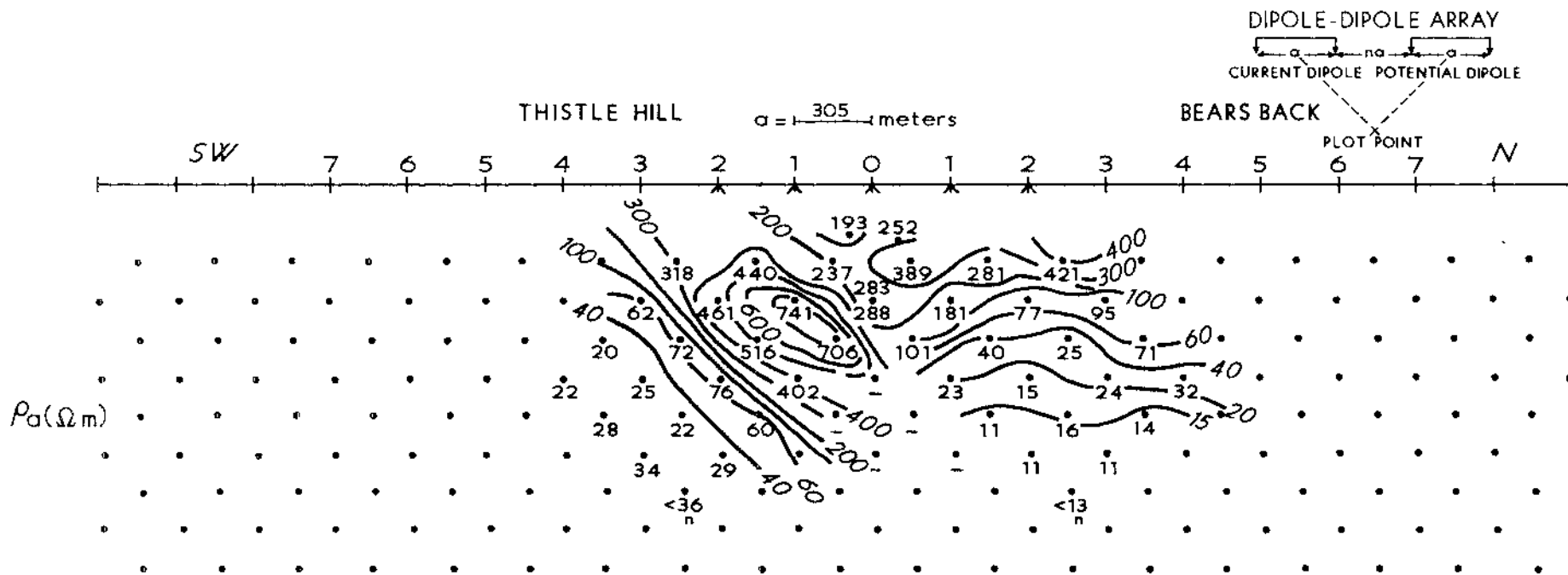


FIGURE 4
 LINE 3
 DIPOLE-DIPOLE ARRAY—APPARENT RESISTIVITY
 TRANSMITTER: ELLIOT M15 RECEIVER: FLUKE
 ASCENSION ISLAND, SOUTH ATLANTIC



DATA BY
 H. P. ROSS and D. J. GREEN
 JUNE 19, 1983

(greater depth).

Plate II shows the numerical model interpretation for lines 2 and 3. This is a complex resistivity distribution and probably indicates three-dimensional effects, particularly near Thistle Hill and the flows and structure between the road and Bears Back. Hence the numerical model solution is only a fair approximation to the actual resistivity structure along the line. The high resistivity bodies, which extend well below sea level (as at Thistle Hill), are most logically dense, low porosity intrusives (or low porosity flows?). The 10 ohm-m zone at depth near Bears Back is within two km of the coast and probably indicates sea water intrusion. Low-resistivity bodies south of Thistle Hill indicate a higher water table and possible thermal fluids at moderate depth. The model is not well constrained beyond station 5SW because near-surface data (near separation) were not recorded with the 5-electrode spread.

4.4 Supplemental Resistivity Surveys

Supplemental resistivity surveys completed in September 1984 included two dipole-dipole profiles with electrode separation (a) of 1000 feet, and one additional bipole-dipole (reconnaissance array) transmitter site. The profiles were located to provide added delineation of the central low-resistivity zone, where topographic effects would be moderate and the access most favorable. Following the completion of the two profiles, a 2000-foot length of line 4 (station 1W to 1E) was used as a transmitting dipole to examine lateral resistivity structure in the vicinity of the two dipole-dipole profiles. The positions of the survey lines and Tx6 receiver sites are shown on Figure 5.

Line 4 is centered (Sta. 0) 500 feet west of the LDTGH drill hole and trends N68°E and S80°W from this point. Topography is severe along the eastern portion of the line. Apparent resistivity decreases rapidly with

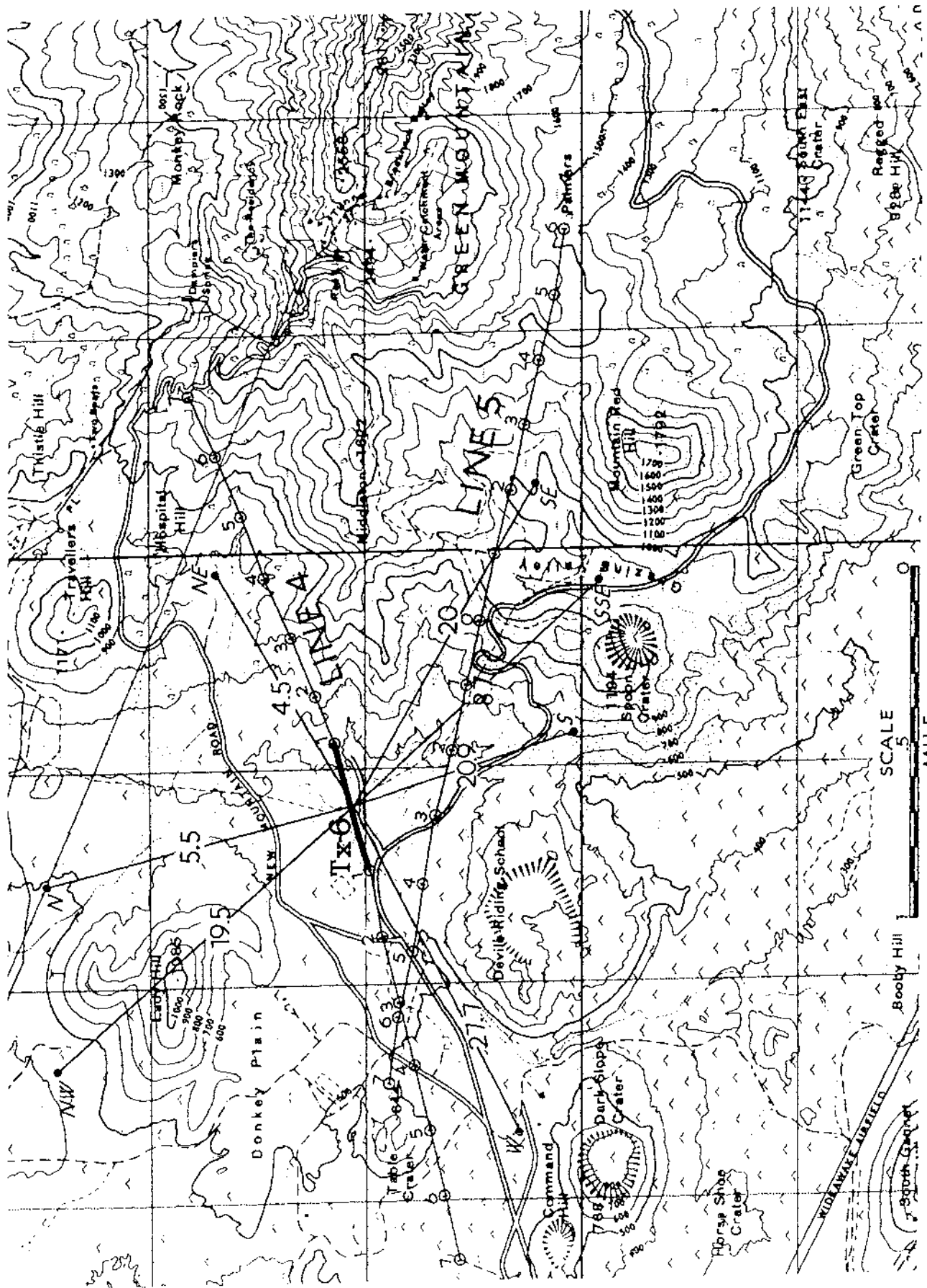


Figure 5. Location map, Line 4 and Line 5, and Tx-6 receiver sites.

increasing separation (depth) (Figure 6). A coherent pattern of 7 to 13 ohm-m values is observed east of center for separations of $n = 3,4,5,6,7$.

Line 5 is centered (Sta. 0) approximately 150 feet west of a ridge which terminates the west margin of Grazing Valley. The line trends $S75^{\circ}E$ from station 0 and $N75^{\circ}W$ from station 0. The data, shown in Figure 7, again suggest a roughly layered resistivity structure with high near-surface resistivities and 6 to 15 ohm-m apparent resistivities at $n = 5,6,7$.

Topography is severe east of station 2W and qualitative interpretation is therefore imprecise.

Bipole-dipole Transmitter 6. Reconnaissance resistivity values were obtained at seven sites around Tx-6. Low resistivity values of 5.5 ohm-m recorded at station 6-N and 4.5 ohm-m recorded at 6-NE are very significant. When considered with the previous reconnaissance data and the dipole-dipole lines, these data can improve the delineation of the low-resistivity zone. The integrated interpretation yields a delineation of the principal low-resistivity zone as shown in Figure 8. Here resistivities somewhat below the 15 ohm-m sub sea level value are delineated, and are inferred to be associated with a geothermal system.

4.5 Numerical Model Interpretation

A substantial effort in numerical modeling was required to support an interpretation of the profile data. Program IP2D (Killpack and Hohmann, 1979) was used to simulate the topographic relief of lines 4 and 5 and then to determine the subsurface resistivity structure along these profiles. Figures 9 and 10 show the numerical models for lines 4 and 5 which achieved the best fit to the observed data.

Line 4. High resistivity (200-500 ohm-m) rocks characterize most of the region between the topographic surface and sea level east of station 0, while

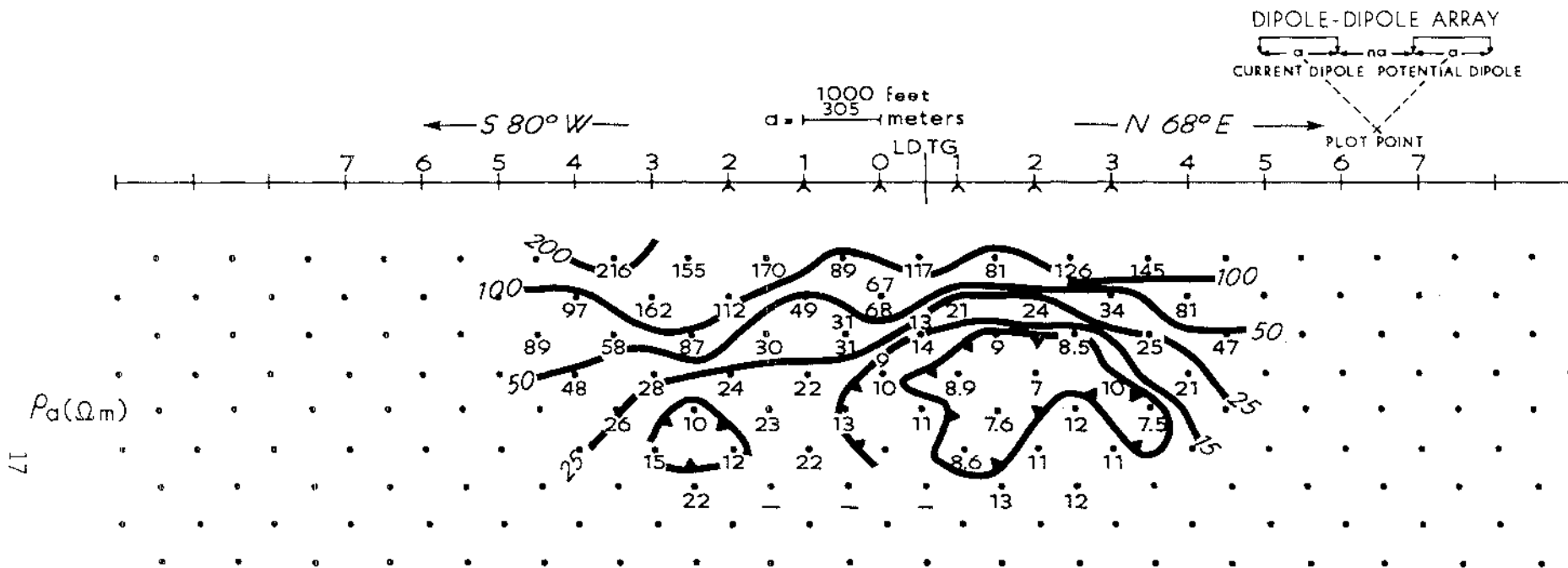
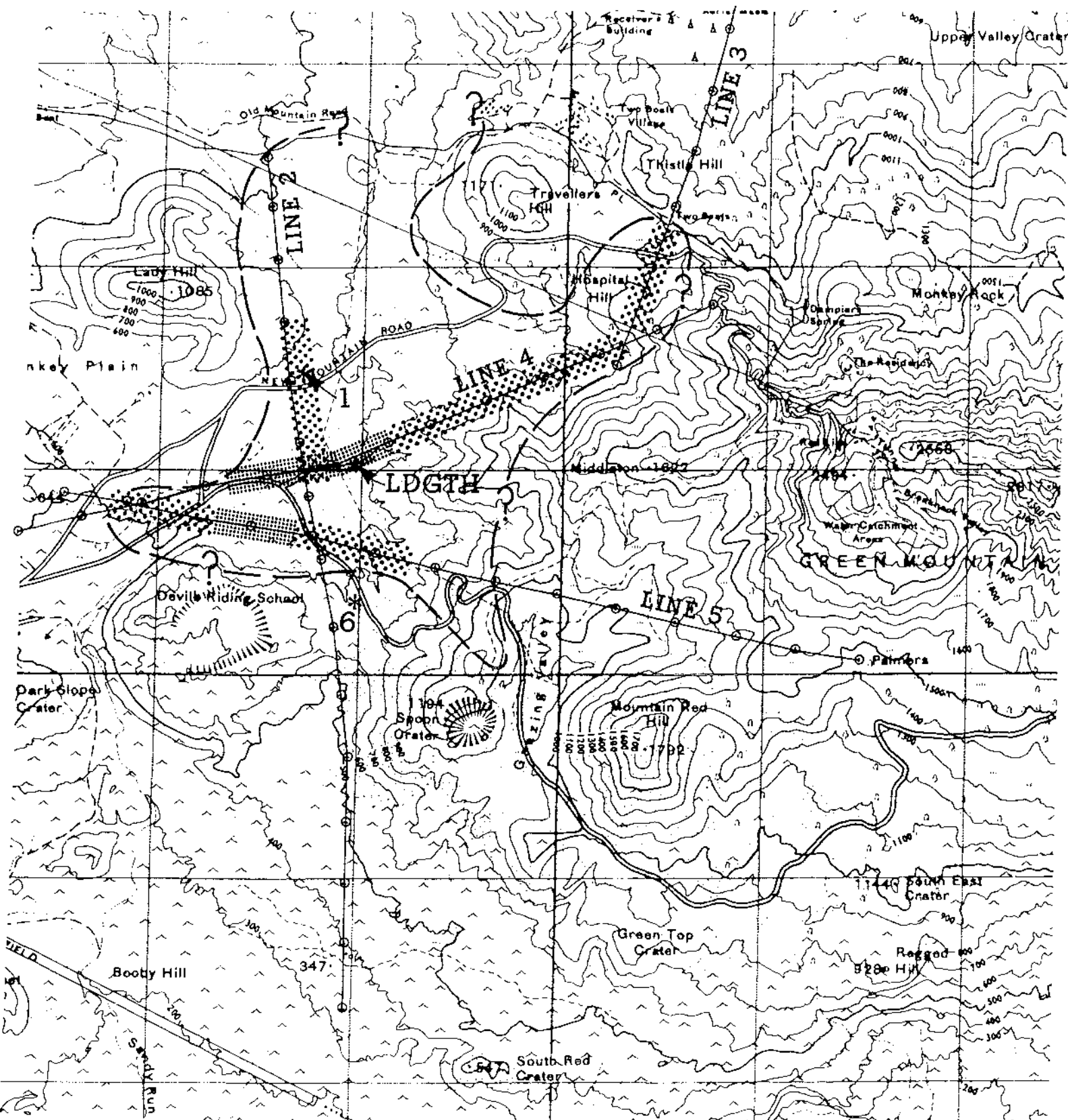


FIGURE 6
LINE 4
DIPOLE-DIPOLE ARRAY—APPARENT RESISTIVITY
TRANSMITTER: ELLIOT M15 RECEIVER: FLUKE
ASCENSION ISLAND, SOUTH ATLANTIC



DATA BY:
C. E. Mackelprang, H. P. Ross





-  Low resistivity zone (s-10 ohm-m) may be thin
-  Low resistivity zone (s-10 ohm-m) greater depth extent

Figure 8. Summary interpretation map, low resistivity zone.

resistive rocks continue to increasingly greater depths (400 to more than 1000 ft) west of the station 0. In order to achieve a satisfactory match to low observed resistivity values (7-12 ohm-m) observed on separations $n = 5,6,7$ a large continuous area of 10 ohm-m was required between stations 1W and 5E which extended to great depth. The residuals (differences between observed and computed resistivity values) for larger separations were significantly reduced by replacing the 10 ohm-m body with a finite depth extent layer of 5 ohm-m, as shown in Figure 9. Attempts to reduce the width of this body by 1500 feet on the east, and then 1500 feet on the west, each led to larger residuals with the observed data and demonstrated substantial sensitivity of the model to geometric changes. Nevertheless we must recognize a level of ambiguity and imprecision, perhaps of the order of the dipole length in dimensions.

Line 5. Figure 10 shows the final best-fit solution for line 5. The extreme topographic variation, modeled here within ± 50 feet, resulted in enhancements of -31 to +36 percent for a uniform earth model. A satisfactory match to $n = 1,2,3$ separations required an irregular above sea level distribution of 100 to 500 ohm-m resistivities. Some minor variation with 15 ohm-m resistivity above sea level, and some 100 ohm-bodies below sea level indicate a departure from a basic 15 ohm-m below sea level model. As in the case of line 4, several (10) larger separation resistivity values achieved a better match to the observed data when a 50 foot thick, 4500 foot wide, 5 ohm-m resistivity zone was emplaced between stations 3W and 5W. Reducing the width of the zone resulted in a deterioration of the match to observed data. Perturbations of the model shown in Figure 10 suggest that a 5 ohm-m zone is present but may not actually be required to match the observed data.

Line 2. A satisfactory model solution for line 2 had been reported in an

earlier study (Ross et al., 1984a). A best fit model for these data indicated an extensive body of 15 ohm-m below sea level, with some resistive bodies continuing to depths of 500-1000 feet below sea level. A 10 ohm-m body of substantial depth extent was required between stations 1E and 4E. This model was replaced with an identical above sea level resistivity structure and a uniform 15 ohm-m body below sea level. The result was a poor fit with 31 larger residuals, 7 smaller residuals, and 6 values unchanged. Although some improvement in fit for the uniform 15 ohm-m below sea level model could be achieved by modifying the entire near surface resistivity structure, it seems most likely that the model of Plate II offers the best solution to the observed data. It is possible, however, that the 10 ohm-m body is not directly beneath the line position, but could be displaced laterally up to 1000 feet from the line. The reconnaissance resistivity data suggest the low-resistivity zone is mainly east of line 2.

Figure 8 presents the integration of dipole-dipole model results and the reconnaissance resistivity data. The most likely region of an anomalous (5-10 ohm-m) low-resistivity zone is an irregularly shaped area of three to five sq km. The departure from 15 ohm-m resistivity subsurface due to sea water migration could readily be explained by geothermal fluids, higher rock and fluid temperatures, associated wall rock alteration, or any combination of these possibilities.

ESL project scientists have discussed the possibility that geothermal fluids rise vertically along structural features within or near the partially defined low-resistivity zone, then move laterally through permeable zones in the subsurface. This geologic model seems most probable, and is somewhat supported by model data. Thus it is quite likely that thermal gradient tests would go through the laterally moving plume and then show a temperature

reversal, unless they are drilled very close to the vertical conduits.

Gradient holes 1, 6, and LDTGH lie within the low resistivity zone and do show anomalous thermal gradients. The resistivity models are inadequate to define the precise location of the vertical conduits.

5.0 SUMMARY AND RECOMMENDATIONS

Two additional dipole-dipole resistivity lines were completed in September. Numerical modeling of these data, supplemented by seven reconnaissance resistivity values and data from an earlier survey, indicate the probable existence of a 5 to 10 ohm-m resistivity zone. These low resistivities contrast with a general 15 ohm-m below sea level background, and probably arise from geothermal fluids rising vertically and then moving laterally in permeable units. The present resistivity data have outlined an area of three to five sq km which probably includes the rising geothermal fluids and the less diluted portions of the geothermal fluid plume. The data and their interpretation are not adequate to specify the controlling vertical structures within 500 feet laterally.

ESL geoscientists have considered the relative resolution, cost, time required, and probability of success in locating a narrow (100 m or 330 ft) wide conductive zone within the area already delineated. It seems unlikely that magnetotellurics (MT), controlled source audio MT (CSAMT) or additional resistivity surveys could locate the target zone with certainty and thus give rise to a better drill test location. Therefore, the next step in reservoir definition must be drilling to acquire measurements of temperature, permeability, and fluid composition of the geothermal resource which has been defined by the electrical resistivity surveys and previous thermal gradient drilling. We recommend that LDTGH be deepened to approximately 5000 feet to

test this zone. Should the results of this drilling prove successful, production drilling will be recommended.

6.0 ACKNOWLEDGEMENTS

We would like to acknowledge the support and enthusiasm of a number of people and organizations who contributed to the completion of this project. These include Michael Nasr and Lt. Col. Walter White of the U.S. Air Force as well as William Koslow of Pan American World Services and Wayne Rollins, PAN AM Manager, and his staff on Ascension Island. Eldon Bray represented U.S. DOE/ID during the completion of the field surveys.

7.0 REFERENCES

- Frangos, W., and Ward, S. H., 1980, Bipole-dipole survey at Roosevelt Hot Springs Thermal Area, Beaver County, Utah: Earth Science Laboratory/UURI rept. ESL-43, 60 p.
- Hohmann, G. W., and Jiracek, G. R., 1979, Bipole-dipole interpretation with three-dimensional models: Earth Science Laboratory/UURI rept. ESL-20, 20 p.
- Keller, G. V., Furgerson, R. B., Lee, C. V., Harthill, N., and Jacobson, J. J., 1975, The dipole mapping method: Geophysics, v. 40, p. 451-472.
- Keller, G. V., Skokan, C. K., Skokan, J. J., Daniels, J., Kauahikaua, J. P., Klein, D. P., and Zablocki, C. J., 1977, Geoelectric studies on the east rift, Kilauea Volcano, Hawaii Island: HIG report HIG-77-15, 195 p.
- Killpack, T. J., and Hohmann, G. W., 1979, Interactive dipole-dipole resistivity and IP modeling of arbitrary two-dimensional structures (IP2D Users Guide and Documentation): Earth Science Laboratory/UURI rept. ESL-15, 35 p.
- Nielson, D. L., and Sibbett, B. S., 1982, Technical Report: Geothermal potential of Ascension Island, South Atlantic - Phase I - Preliminary Examination: Earth Science Laboratory/UURI rept. to U.S. Air Force and U.S. DOE/ID, 79 p.
- Nielson, D. L., Sibbett, B. S., Shane, M. K., and Whitbeck, J. F., 1984, Final Report: Geothermal exploration and geothermal power plant update for Ascension Island, South Atlantic Ocean: Report no. DOE/ID/12079-118 to U.S. Air Force and U.S. DOE/ID, 43 p.

- Ross, H. P., Nielson, D. L., and Green, D. J., 1984a, Aeromagnetic map of Ascension Island, South Atlantic Ocean: Earth Science Laboratory/UURI. Tech. rept. to U.S. Air Force and U.S. DOE/ID.
- Ross, H. P., Green, D. J., Sibbett, B. S., and Nielson, D. L., 1984b, Electrical resistivity surveys, Ascension Island, South Atlantic Ocean: Earth Science Laboratory/UURI Tech. rept. to U.S. Air Force and U.S. DOE/ID.
- Stanley, W. D., Jackson, D. B., and Zohdy, A. A. R., 1976, Deep electrical investigations in the Long Valley geothermal area, California: J. Geophys. Res., v. 81, p. 810-820.
- van Andel, T. H., Rea, D. K., von Herzen, R. P., and Hoskins, H., 1973, Ascension Fracture Zone, Ascension Island and the mid-Atlantic Ridge: Geol. Soc. America Bull., v. 84, p. 1527-1546.

APPENDIX I

NUMERICAL MODEL RESULTS

This appendix includes selected computer printouts which document the numerical models and computed apparent resistivities for selected solutions to the data of dipole-dipole lines 2, 4, and 5. Comparison with the observed data for these lines, shown as Figures 3, 6, and 7 respectively will allow an independent judgement of the goodness-of-fit to the observed data. An evaluation of the topographic effects on lines 4 and 5 is also provided.

Dipole - Dipole Line 4 a = 1000 ft (305 m)

File #2	Topographic model, uniform earth
File #30	Large 10 ohm-m body
File #36	5 ohm-m body, station 0-5E
File #40	5 ohm-m body, station 1.5W-5E: <u>SOLUTION</u>
File #41	5 ohm-m body, station 1.5W-3.5E

Dipole-Dipole Line 5 a = 1000 ft (305 m)

File #3	Topographic model, uniform earth
File #38	15 ohm-m at depth
File #39	5 ohm-m body, station 5W-4W
File #44	5 ohm-m body, station 6.5W-2.5E: <u>SOLUTION</u>

Dipole-Dipole Line 2 a = 1000 ft (305 m)

File #42	10 ohm-m body, station 1.5-4N: <u>SOLUTION</u>
FILE #43	Uniform 15 ohm-m below sea level

LINE 4

MEDIA RESISTIVITY (OHM-METERS)

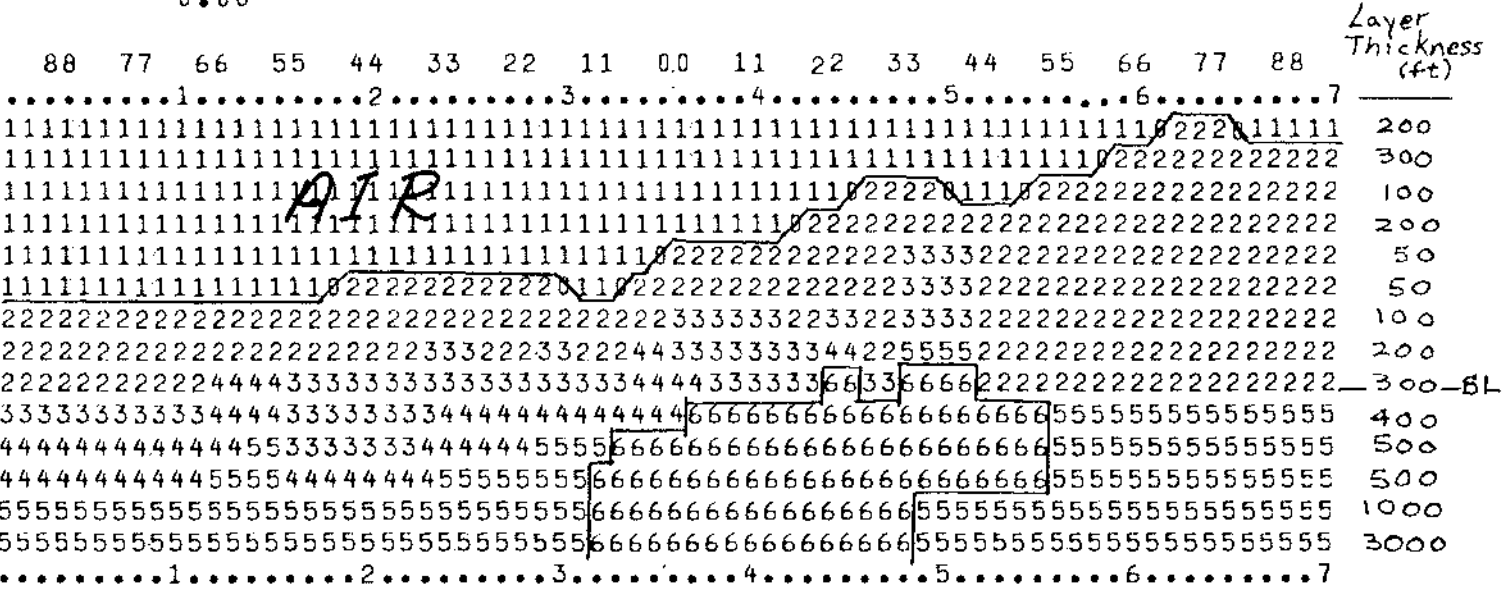
100000.00 500.00 200.00 100.00 15.00

10.00

MEDIA PFE (%)

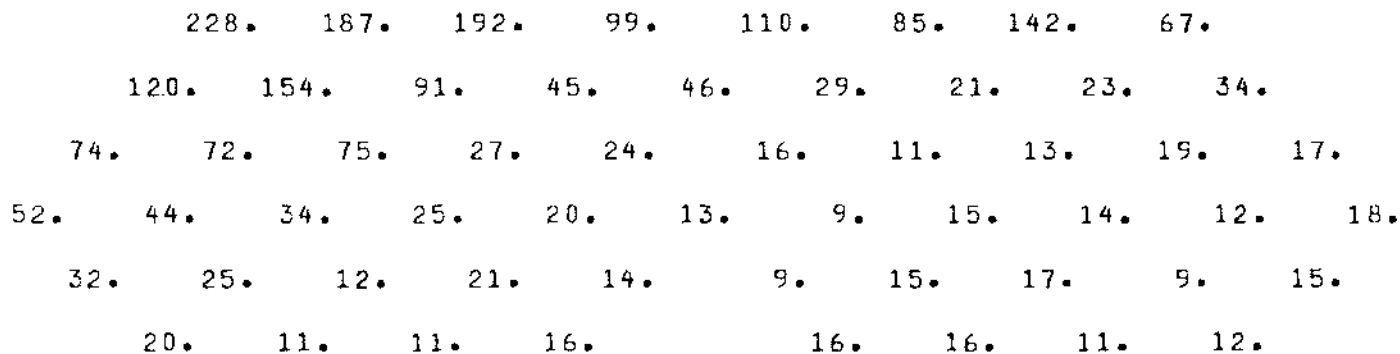
0.00 0.00 0.00 0.00 0.00

0.00



APPARENT RESISTIVITY (CALCULATED)

-5 -4 -3 -2 -1 0 +1 +2 +3 +4 +5



ASCENSION ISLAND, SOUTH ATLANTIC

LINE 4

MEDIA RESISTIVITY (OHM-METERS)

1000.00	500.00	200.00	100.00	15.00
10.00	5.00			
MEDIA PFE (%)				
0.00	0.00	0.00	0.00	0.00
0.00	0.00			

88	77	66	55	44	33	22	11	00	11	22	33	44	55	66	77	88	Layer Thickness
1	1	1	1	1	1	1	1	1	1	1	1	1	1	1	1	1	200
1	1	1	1	1	1	1	1	1	1	1	1	1	1	1	1	1	300
1	1	1	1	1	1	1	1	1	1	1	1	1	1	1	1	1	100
1	1	1	1	1	1	1	1	1	1	1	1	1	1	1	1	1	200
1	1	1	1	1	1	1	1	1	1	1	1	1	1	1	1	1	50
1	1	1	1	1	1	1	1	1	1	1	1	1	1	1	1	1	50
2	2	2	2	2	2	2	2	2	2	2	2	2	2	2	2	2	100
2	2	2	2	2	2	2	2	2	2	2	2	2	2	2	2	2	200
2	2	2	2	2	2	2	2	2	2	2	2	2	2	2	2	2	300
3	3	3	3	3	3	3	3	3	3	3	3	3	3	3	3	3	400
4	4	4	4	4	4	4	4	4	4	4	4	4	4	4	4	4	500
4	4	4	4	4	4	4	4	4	4	4	4	4	4	4	4	4	500
5	5	5	5	5	5	5	5	5	5	5	5	5	5	5	5	5	1000
5	5	5	5	5	5	5	5	5	5	5	5	5	5	5	5	5	3000

APPARENT RESISTIVITY (CALCULATED)

-5	-4	-3	-2	-1	0	+1	+2	+3	+4	+5
228.	187.	193.	99.	106.	84.	144.	68.			
120.	154.	93.	46.	42.	26.	19.	17.	30.		
74.	72.	79.	29.	22.	15.	10.	9.	13.	14.	
51.	45.	37.	28.	18.	11.	8.	15.	12.	9.	14.
32.	28.	14.	18.	12.	8.	15.	21.	9.	11.	
23.	13.	9.	13.		15.	21.	16.	12.		

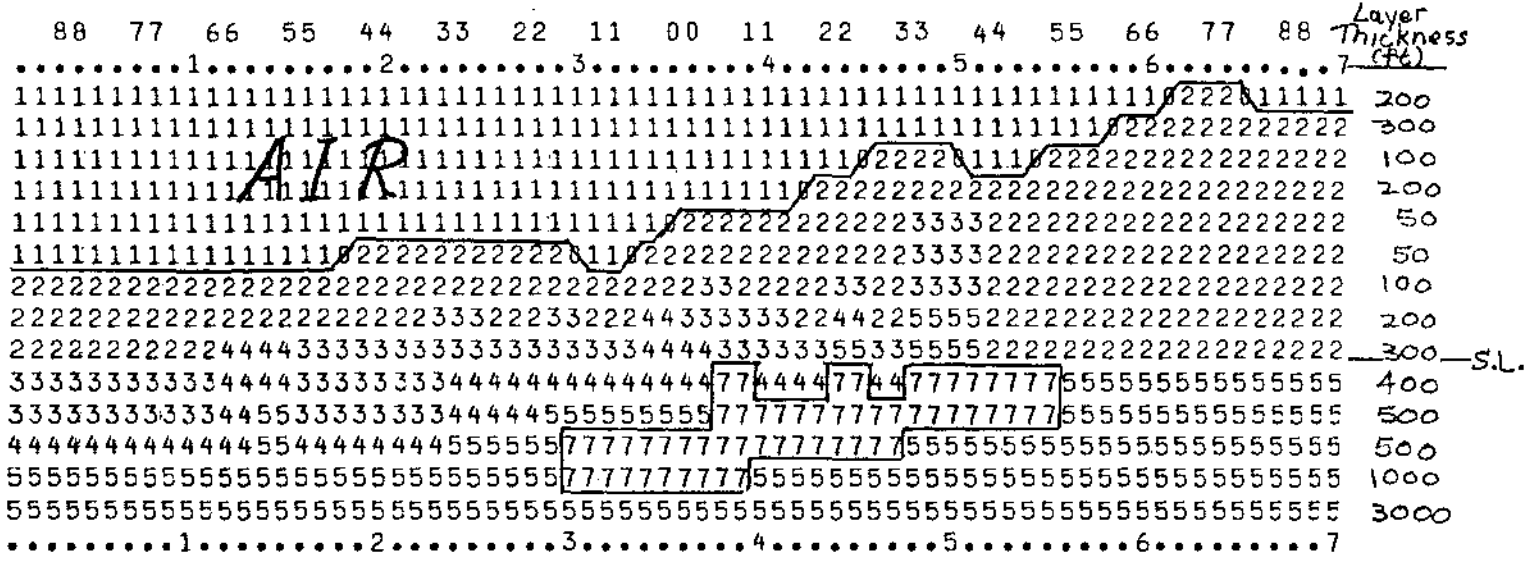
File #36 5 ohm-m body, station 0-5E

MEDIA RESISTIVITY (OHM-METERS)

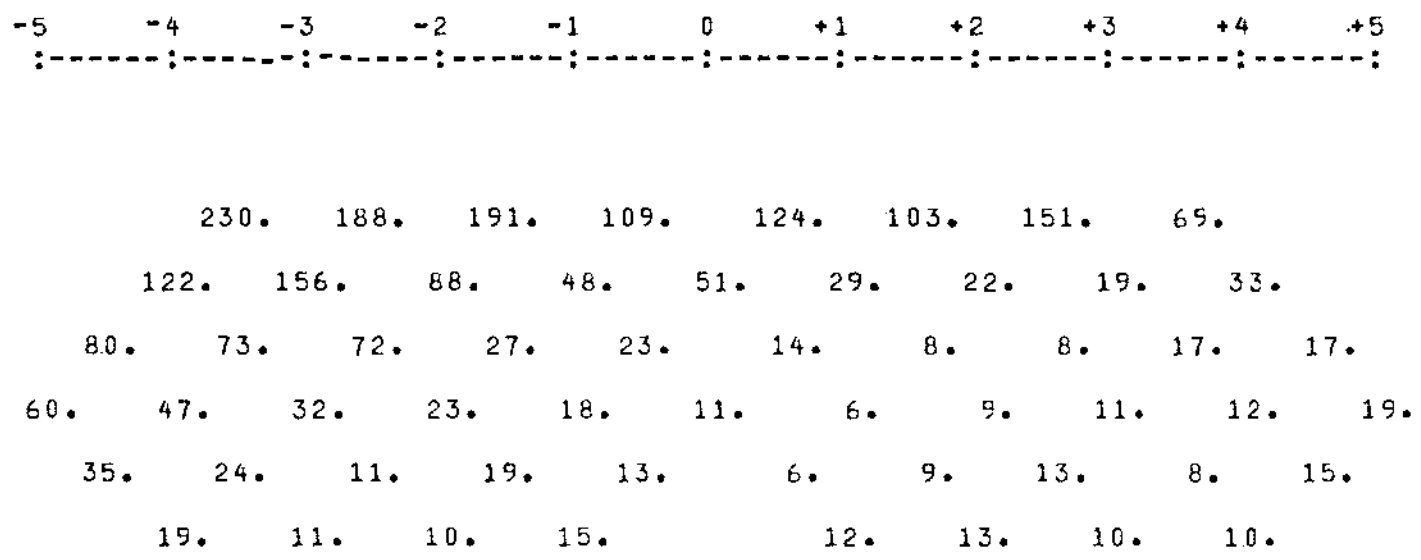
100000.00	500.00	200.00	100.00	15.00
10.00	5.00			

MEDIA PFE (%)

0.00	0.00	0.00	0.00	0.00
0.00	0.00			



APPARENT RESISTIVITY (CALCULATED)



File #40 5 ohm-m body, station 1.5W-5E: SOLUTION

ASCENSION ISLAND , SOUTH PACIFIC
 LINE 5
 MEDIA RESISTIVITY (OHM-METERS)
 1000.00.00 100.00
 MEDIA PFE (%)
 0.00 0.00

LINE 5 FILE #3
 Topo Model

88	77	66	55	44	33	22	11	00	11	22	33	44	55	66	77	88	Layer Thickness (ft)
1	1	1	1	1	1	1	1	1	1	1	1	1	1	1	1	1	100
1	1	1	1	1	1	1	1	1	1	1	1	1	1	1	1	1	100
1	1	1	1	1	1	1	1	1	1	1	1	1	1	1	1	1	200
1	1	1	1	1	1	1	1	1	1	1	1	1	1	1	1	1	200
1	1	1	1	1	1	1	1	1	1	1	1	1	1	1	1	1	100
1	1	1	1	1	1	1	1	1	1	1	1	1	1	1	1	1	150
1	1	1	1	1	1	1	1	1	1	1	1	1	1	1	1	1	100
1	1	1	1	1	1	1	1	1	1	1	1	1	1	1	1	1	100
2	2	2	2	2	2	2	2	2	2	2	2	2	2	2	2	2	100
2	2	2	2	2	2	2	2	2	2	2	2	2	2	2	2	2	200
2	2	2	2	2	2	2	2	2	2	2	2	2	2	2	2	2	300
2	2	2	2	2	2	2	2	2	2	2	2	2	2	2	2	2	400
2	2	2	2	2	2	2	2	2	2	2	2	2	2	2	2	2	500
2	2	2	2	2	2	2	2	2	2	2	2	2	2	2	2	2	500
2	2	2	2	2	2	2	2	2	2	2	2	2	2	2	2	2	1000
2	2	2	2	2	2	2	2	2	2	2	2	2	2	2	2	2	3000

APPARENT RESISTIVITY (CALCULATED)

-5 -4 -3 -2 -1 0 +1 +2 +3 +4 +5
 :-----:-----:-----:-----:-----:-----:-----:-----:-----:-----:-----:

		100.	91.	94.	90.	105.	94.	59.	136.	
	104.	96.	92.	92.	116.	106.	59.	103.	124.	
106.	98.	92.	88.	116.	119.	65.	89.	101.	138.	
107.	99.	92.	86.	108.	121.	73.	93.	87.	116.	138.
	100.	92.	86.	105.	113.	74.	100.	90.	98.	118.
		91.	85.	103.	109.		99.	96.	101.	100.

File #3 Topographic model, uniform earth

ASCENSION ISLAND, SOUTH ATLANTIC
LINE 5

61112 1 Feb 13
P. 15.00

MEDIA RESISTIVITY (OHM-METERS)	10000.00	500.00	200.00	100.00	15.00
MEDIA PFE (%)	0.00	0.00	0.00	0.00	0.00

	88	77	66	55	44	33	22	11	00	11	22	33	44	55	66	77	88	Layer Thickness
1	1	1	1	1	1	1	1	1	1	1	1	1	1	1	1	1	1	100
2	1	1	1	1	1	1	1	1	1	1	1	1	1	1	1	1	1	100
3	1	1	1	1	1	1	1	1	1	1	1	1	1	1	1	1	1	200
4	1	1	1	1	1	1	1	1	1	1	1	1	1	1	1	1	1	100
5	1	1	1	1	1	1	1	1	1	1	1	1	1	1	1	1	1	150
6	1	1	1	1	1	1	1	1	1	1	1	1	1	1	1	1	1	100
7	1	1	1	1	1	1	1	1	1	1	1	1	1	1	1	1	1	100
8	1	1	1	1	1	1	1	1	1	1	1	1	1	1	1	1	1	200
9	1	1	1	1	1	1	1	1	1	1	1	1	1	1	1	1	1	300
10	1	1	1	1	1	1	1	1	1	1	1	1	1	1	1	1	1	400
11	1	1	1	1	1	1	1	1	1	1	1	1	1	1	1	1	1	500
12	1	1	1	1	1	1	1	1	1	1	1	1	1	1	1	1	1	500
13	1	1	1	1	1	1	1	1	1	1	1	1	1	1	1	1	1	1000
14	1	1	1	1	1	1	1	1	1	1	1	1	1	1	1	1	1	3000

APPARENT RESISTIVITY (CALCULATED)

-5	-4	-3	-2	-1	0	+1	+2	+3	+4	+5
82.	93.	216.	171.	204.	156.	131.	174.			
20.	38.	34.	50.	99.	88.	66.	77.	144.		
15.	19.	23.	13.	32.	48.	41.	31.	63.	99.	
16.	18.	12.	12.	16.	21.	35.	20.	27.	45.	60.
21.	12.	7.	18.	15.	19.	20.	21.	21.	32.	
14.	7.	11.	18.		11.	26.	20.	17.		

File #38 15 ohm-m at depth

LINE 5

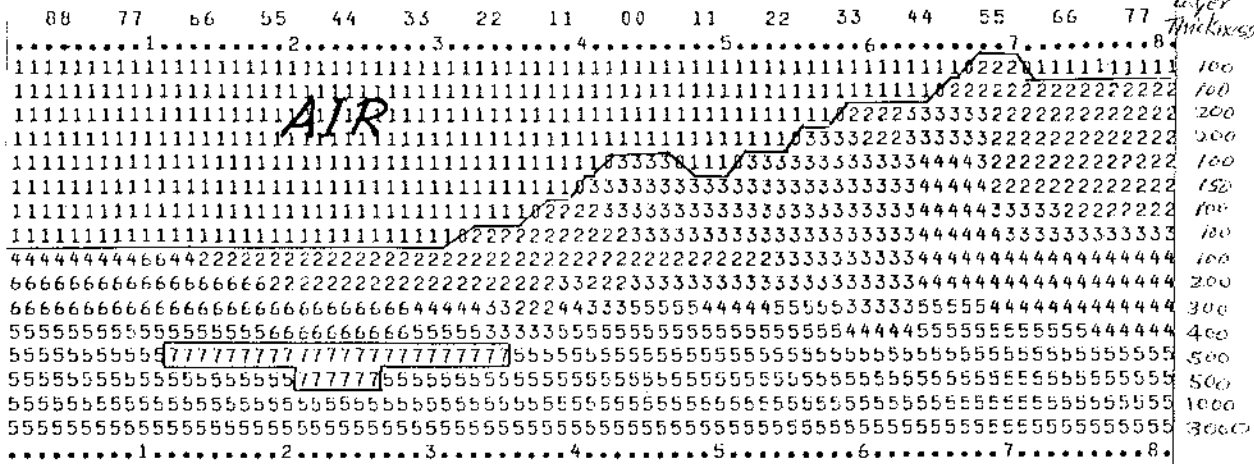
MEDIA RESISTIVITY (OHM-METERS)

100000.00 500.00 200.00 100.00 15.00

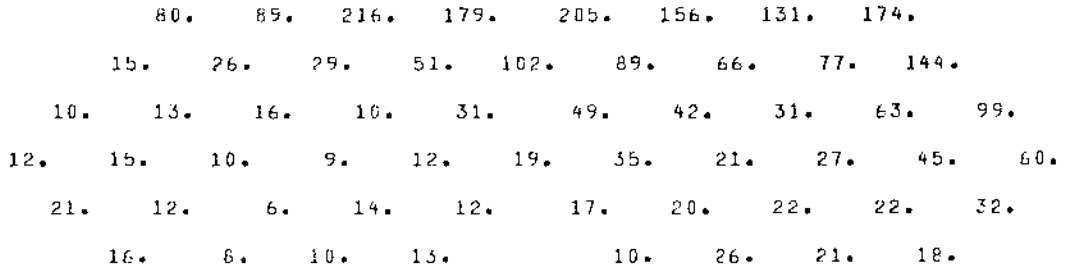
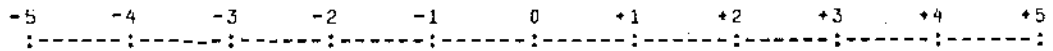
50.00 5.00

MEDIA PFL (%)

0.00 0.00 0.00 0.00 0.00



APPARENT RESISTIVITY (CALCULATED)



File #44 5 ohm-m body, station 6.5W-2.5E: SOLUTION

